

# FAST PARTICLE CONFINEMENT AND COLLECTIVE EFFECTS IN NSTX

N. N. Gorelenkov

*in collaboration with*

E. Belova, C. Z. Cheng, D. Darrow, E. Fredrickson, W.W. Heidbrink

G. J. Kramer, R. Nazikian, M. Redi, R. White, V. Yavorski

*Princeton Plasma Physics Laboratory*

## Outline

---

### 1. Single particle confinement

(a) First orbit losses

(b) Stochastic losses

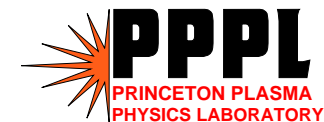
### 2. Collective effects in NSTX :

(a) Global/Compressional Alfvén eigenmodes

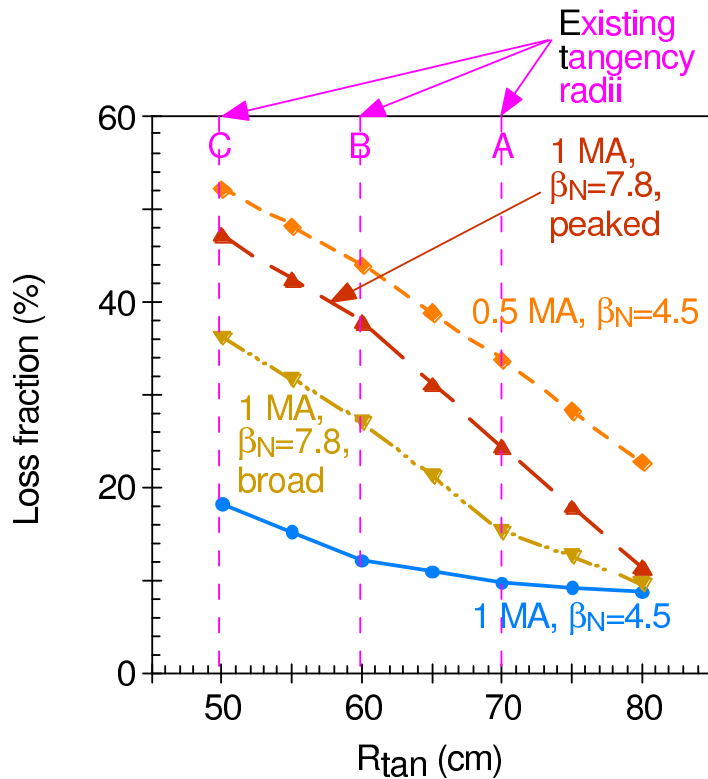
(b) Toroidicity induced Alfvén eigenmodes

(c) Ion bounce frequency fishbones

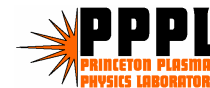
8th International ST Workshop, PPPL, November 18-21, 2002.



# Loss fraction increases rapidly as beam tangency radius is reduced



- Beam line A ( $R_{\text{tan}} = 69.2$  cm) is best confined
- Global confinement trends should be evidenced in loss measurements and in beam “blip” experiments



*Eigol code, D. Darrow*

# Collisionless Fast Ion Loss: NSTX Equilibria

---

## CONBEAM

For NSTX equilibria  $0.6 < I_p < 1 \text{ MA}$ ,  $0.3 < B_T < 0.45 \text{ T}$ ,  
losses of 10% to 50%;  
best confinement at high  $I_p$ ,  $B_T$  and small  $\rho_L$ .

## GYROXY and EIGOL

NSTX 23%  $\beta$  equilibrium

Benchmarked for an 80 KeV, 0.5 m tangency radius beam

Excellent agreement at short times:

21% of 54,000 ions lost after  $\sim 7.5 \times 10^5$  sec.

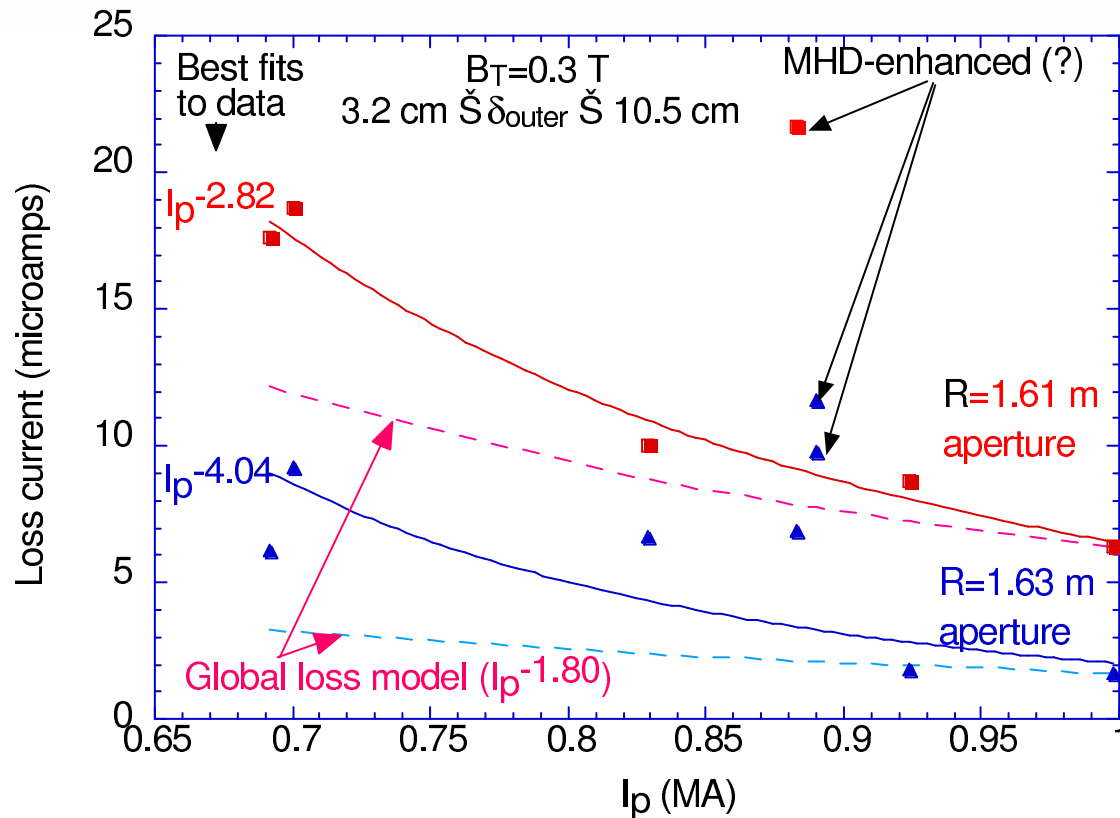
**GYROXY:** After x10 longer orbit time ( $\tau_{\text{slow}}/20$ ), 26% loss

**CONBEAM:** 26% loss

*Codes comparison, M. Redy*



# Loss varies with $I_p$ more strongly than global model predicts



- Difficult to get MHD-free plasma at low  $I_p$
- Variation of local loss could differ from global prediction

*Lost probe, D. Darrow*

## Summary of Ion Confinement Observations

---

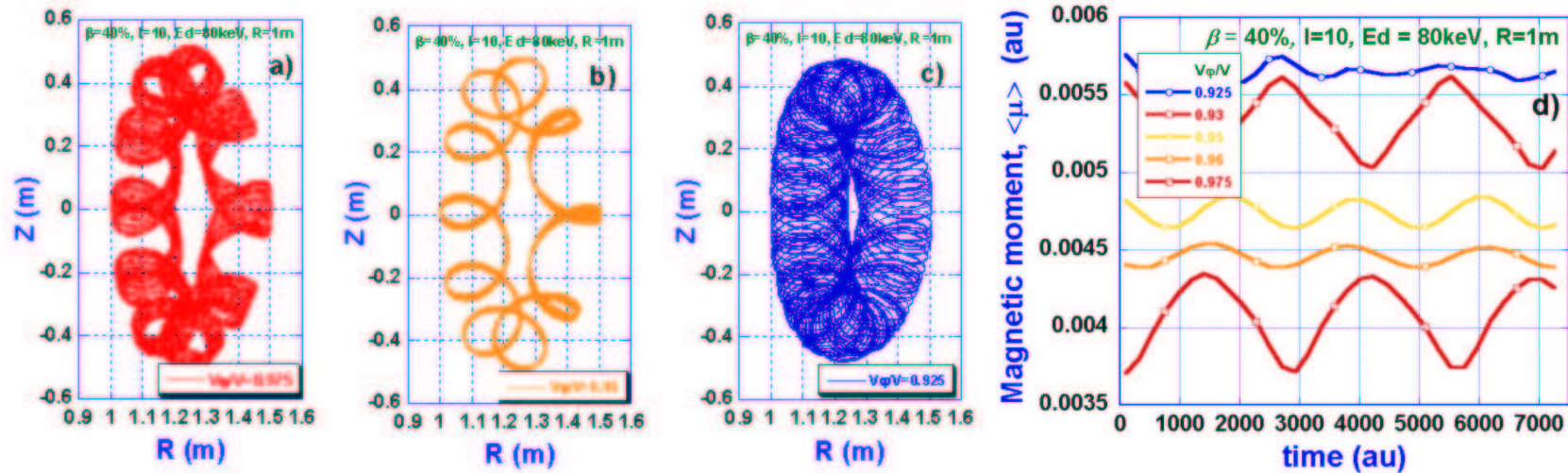
PPPL

Loss ion probe and other diagnostics: NPA, neutron detectors conclude:

- ✓ Fast ion confinement in quiescent NSTX plasmas appears classical within  $\sim 25\%$  error bars:
  1. prompt orbit losses
  2. collisional slowing down and scattering
- ✓ MHD can have strong effects on beam ion confinement, *with 90% shots having some MHD activity affecting neutron rate.*
- ✓ see APS and IAEA 2002 by D. Darrow, *et.al.*

# New physics of nonadiabatic ion motion in NSTX

PPPL



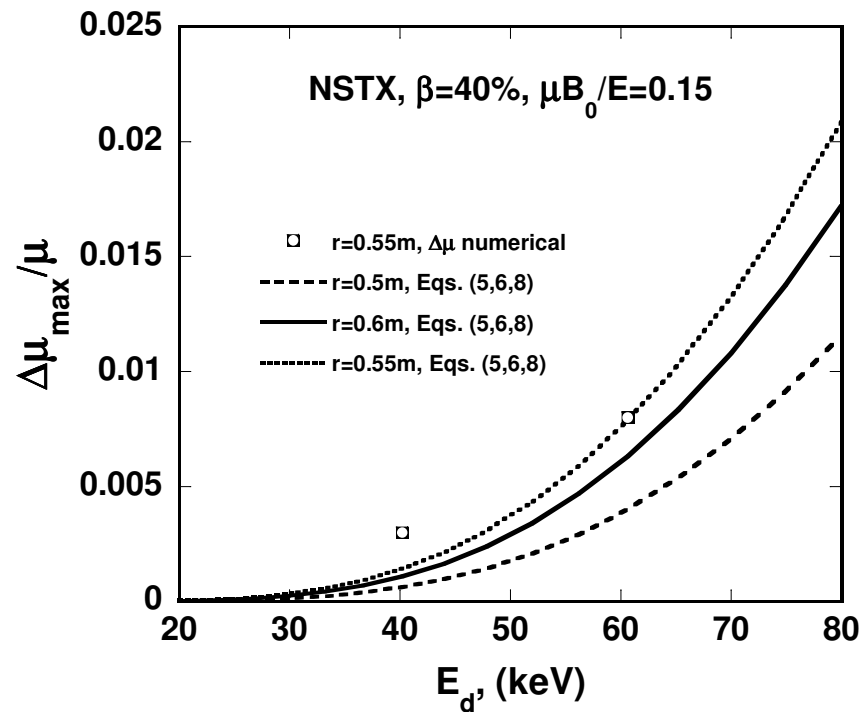
Large variation in  $\langle \mu \rangle$  is expected in NSTX up to  $\Delta \langle \mu \rangle \sim \langle \mu \rangle$ .

May result in stochastic radial diffusion.

V. Yavorski, EPS-2001, IAEA - 2002. (also theory by Kolesnichenko *et.al.*, 02)

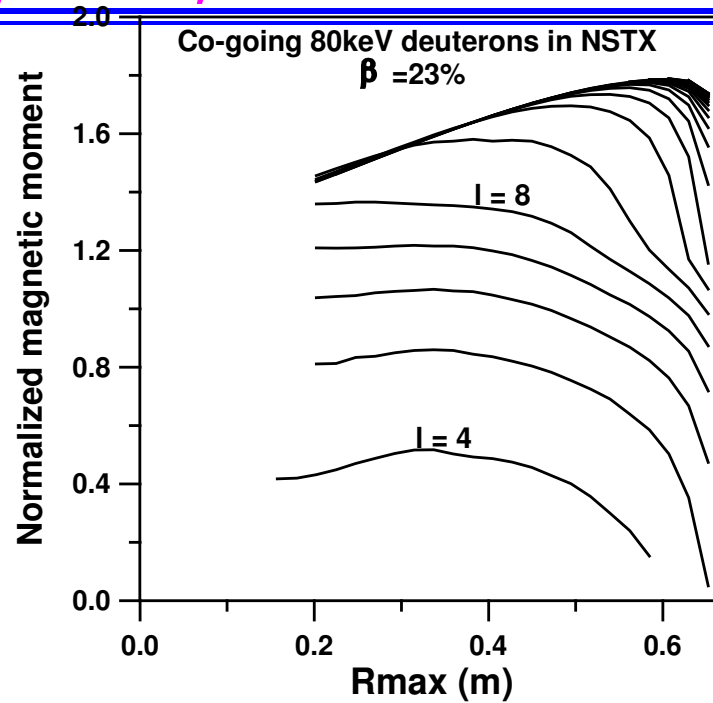
## Theory of $\mu$ change agrees with calculations

PPPL



- ✓ Low energies shows unusually high  $\mu$  oscillations.
- ✓ Analysis shows that high harmonics in equilibrium are the reason  $\delta B/B \sim 10^{-3} - 10^{-2}$ .
- ✓ May result in new mechanisms of wave - particle interaction.

*Nonadiabatic ion motion resonances cover wide regions in phase space in NSTX*



PPPL

Fig. 6



## Collective Effects: High Frequency Instability Observations

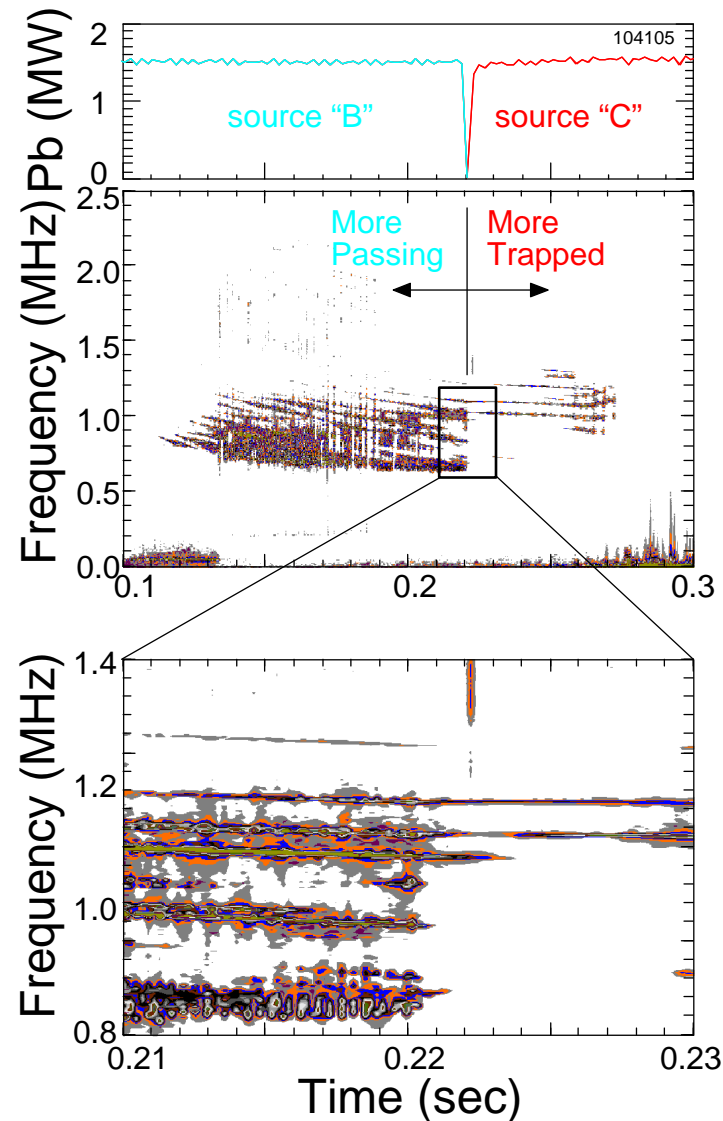
PPPL

1. Multiple sub-ion cyclotron frequency instabilities were observed in NSTX.
2. Frequency *typically* scales with **Alfvén speed**, but not always.
3. Instability is driven by **fast super Alfvénic ions**,  $v_{b0} \simeq 3v_A$  due to  $80keV$  NBI.
4. *Typically* the frequency spectrum has “**bunches**” of peaks almost evenly spaced in frequency. There are **multiple peaks** within each bunch.
5. Instability is sensitive to the injection angle of different tangential NBI sources having tangential radius  $R_{tan} = 69.4, 59.2, \text{ and } 48.7 \text{ cm}$  (from more passing to more trapped).
6. Instability has dependence on energy distribution.
7. Theory motivation
  - ✓ Are they CAEs? HYM shows shear Alfvén polarization (see next, Elena’s talk), GAEs?
  - ✓ AEs can be used for **energy channeling** from fast ions to electrons and ions?
  - ✓ Instability can be used to diagnose plasma edge: rotation, fast particles.

## Sub-Cyclotron Instability - CAE Observed in NSTX

PPPL

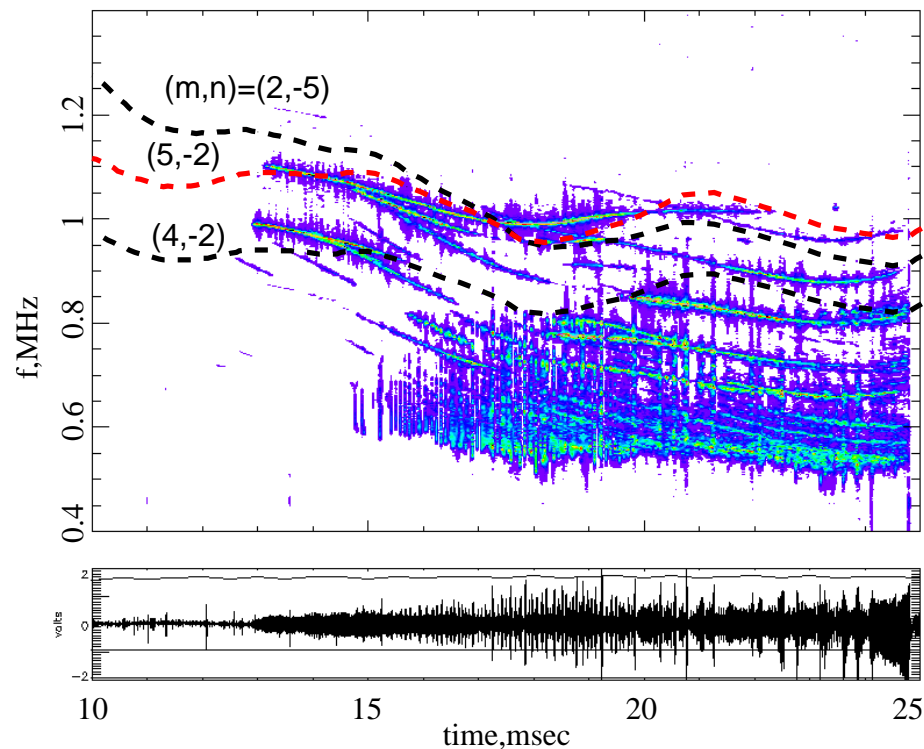
- ✓ Instabilities are coherent modes driven by NBI.
- ✓ Some modes persist through the NBI source switch.
- ✓ Sensitive to NBI injection angle.
- ✓ Modes are identified as Compressional Alfvén Eigenmodes.
- ✓ The same time evolution of peak frequencies. Fredrickson '01, Gorelenkov '02.



## New Features of Sub-Cyclotron Instability Spectrum

PPPL

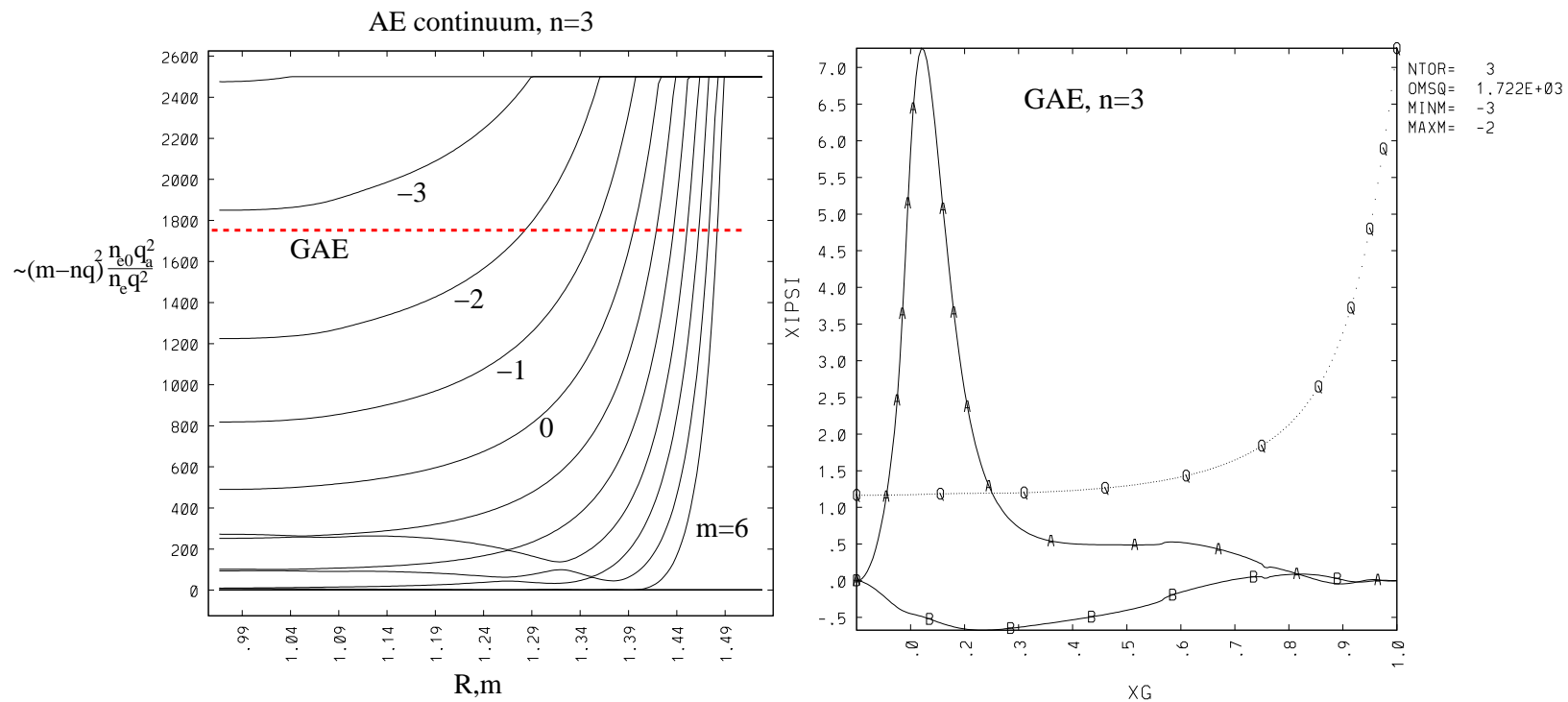
Dashed curves are **GAE dispersion**  $\omega_{GAE} \simeq v_{A0}(m - nq_0)/q_0R$ .



- ✓ Observed frequencies of different  $(m, n)$  modes intersect  
⇒ characteristic of shear Alfvén Eigenmodes.
- ✓ We identify these new modes as Global Alfvén Eigenmodes (GAE),  
(APPERT, 1982).

# GAE Radial Structure is close to cylindrical, single $m$

PPPL



damping on the continuum is dominant

$\sim e^{-m}$ , higher  $m$ 's are less stable.

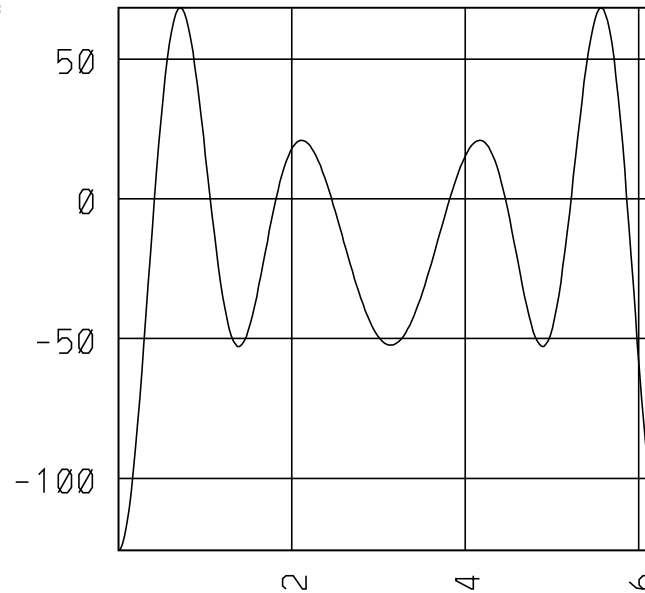
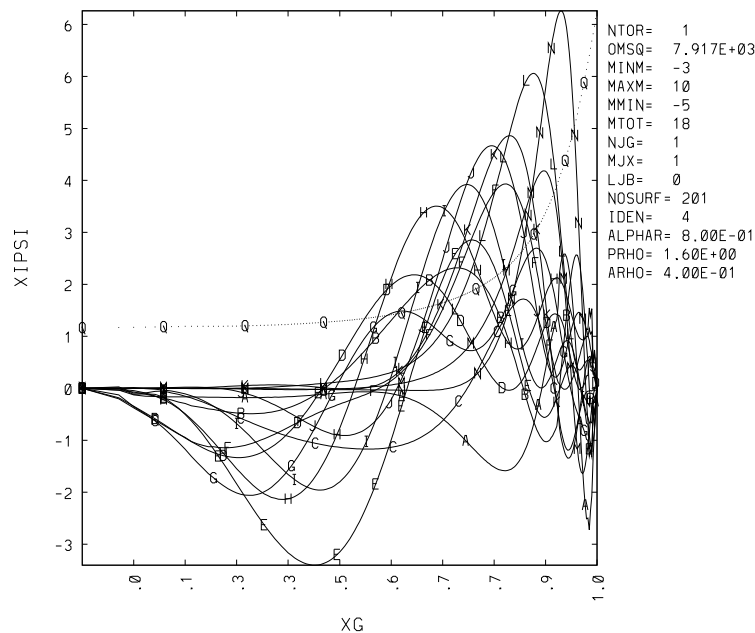
Such GAEs were studied by Appert, '82:

$$\omega = k_{\parallel} v_{A0} \simeq \left( \frac{m}{q_0} - n \right) \frac{v_{A0}}{R_0}.$$

## CAE Radial Structure is Localized at LFS

PPPL

Plasma radial displacement ( $\sim E_\theta \sim \partial E_r / \partial r$  for ideal MHD part) and parallel poloidal variation of perturbed magnetic field at half of minor radius



Use this  $m = 4$ ,  $s = 0$ , we have  $f = 1.45 MHz$  and  $\omega a / v_{A0} = 9.4$  in low beta NSTX equilibrium vs. our theoretical prediction of  $\omega a / v_A \simeq 8$ .

## CAE variational solution and dispersion

PPPL

With density given by  $n = n_0(1 - r^2)^\sigma$ , at  $r_0/a = \sqrt{1/(1 + \sigma)}$ :

$$\omega_0 = \frac{v_{A0}}{r_0 \kappa} \left[ (2m + 1) \sqrt{\epsilon_0 - \alpha_0} + 2(2s + 1) \kappa \sqrt{\frac{1 + \sigma}{2\sigma}} + \frac{n^2 r_0^2 \kappa^2}{R^2 (2m + 1) \sqrt{\epsilon_0 - \alpha_0}} \right],$$

where  $\alpha_0 = B_\theta^2/2B_\phi^2$  and all quantities are estimated at  $r = r_0$ ,  $\theta = 0$ .

Instabilities with different  $m$ 's are separated in frequency by

$$\Delta f_m \simeq \frac{2v_A}{2\pi\kappa r} \sqrt{\epsilon_0 - \alpha_0} < \Delta f_s \simeq \frac{v_A}{2\pi\kappa r} \sqrt{\frac{2(1 + \sigma_i)}{\sigma_i}}.$$

✓ NSTX shot #103701  $B_{r=r_0} = 0.27T$ ,  $r = 0.5m$ , elongation  $\kappa = 1.6$ ,  $n_e = 2 \times 10^{13} cm^{-3}$  (TRANSP).

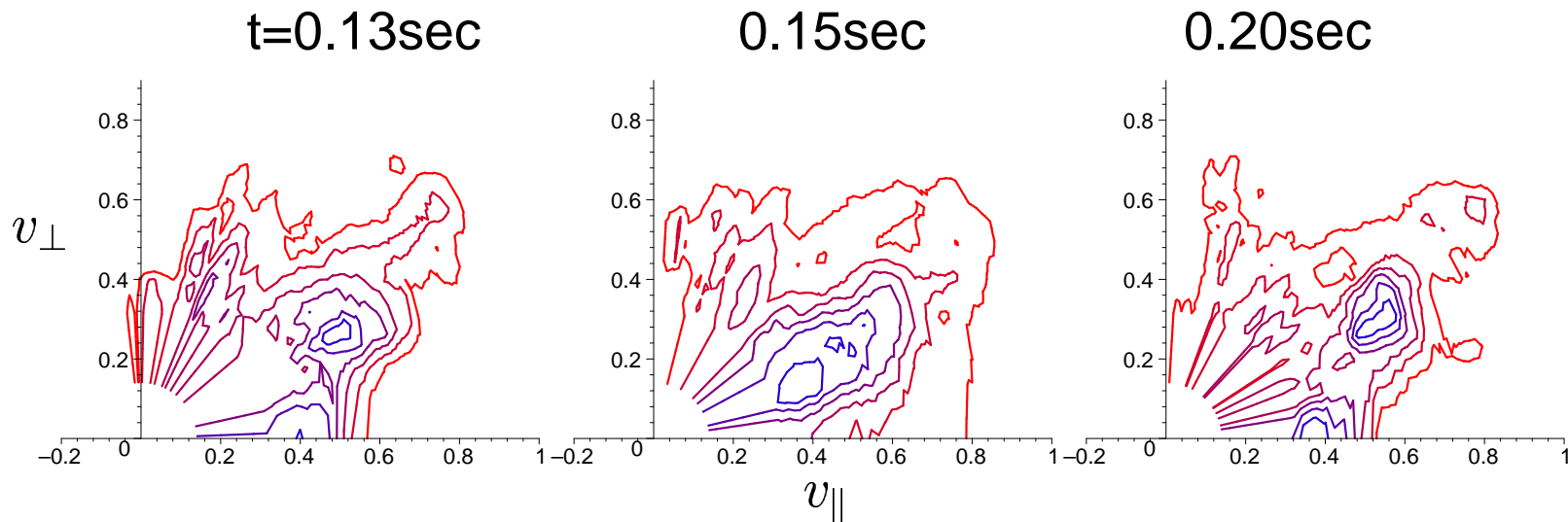
Use also parameter:  $\epsilon_0 = r/(R_0 + r) = 0.3$ ,  $\alpha_0 = 1/8$ :  $\Delta f_m = 150kHz$ ,  $\Delta f_s = 1.1MHz$ .

For #103431  $B = 0.32T$ ,  $n_e = 4 \times 10^{13} cm^{-3}$ ,  $\Delta f_m = 125kHz$ ,  $\Delta f_s = 1MHz$ .

✓ Observed  $\Delta f_m \simeq 120kHz$  in #103701 and  $\Delta f_m \simeq 110kHz$  in #103431 with the  $\Delta f_s \simeq 1MHz$

*TRANSP shows close to “double” single pitch angle NBI distribution function*

PPPL



- ✓ Shown is the distribution function at the LFS,  $r/a=0.5$ .
- ✓ Often distribution function may be casted into the “trapped” and “passing” parts, i.e. confined at the edge and at HFS tangential surface.
- ✓ At fixed  $v_{\parallel}$  positive velocity space gradient drives instability.

## Comparison of CAE and GAE properties

PPPL

mode →	CAE	GAE
dispersion	$\omega = kv_A \simeq mv_A/\kappa r$	$\omega = k_{\parallel 0} v_{A0}$
localization	LFS, plasma edge, $r/a \geq 1/2$	plasma center
resonance $v_{\parallel}$	$\frac{v_{\parallel}}{v_A} \geq \frac{k_{\perp}}{k_{\parallel}} \left( \frac{\omega_c}{\omega} - 1 \right)$	$\frac{v_{\parallel}}{v_A} \geq \frac{\omega_c}{\omega} - 1$
$k_{\parallel}$	$k_{\parallel} \simeq (\omega_c - \omega) / v_{\parallel b}, k_{\parallel} > 0$	$k_{\parallel} \simeq \omega_c / v_{b0}, k_{\parallel} > 0$
$v_{\perp}$	$\frac{v_{\perp} \omega}{v_A \omega_c} \geq 1$	$\frac{k_{\perp} v_{\perp} \omega}{k_{\parallel} v_A \omega_c} \geq 2$

Cyclotron resonance with beam ions  $\omega - l\omega_{cD} - k_{\parallel} v_{\parallel b} \simeq 0, l = \pm 1$ .

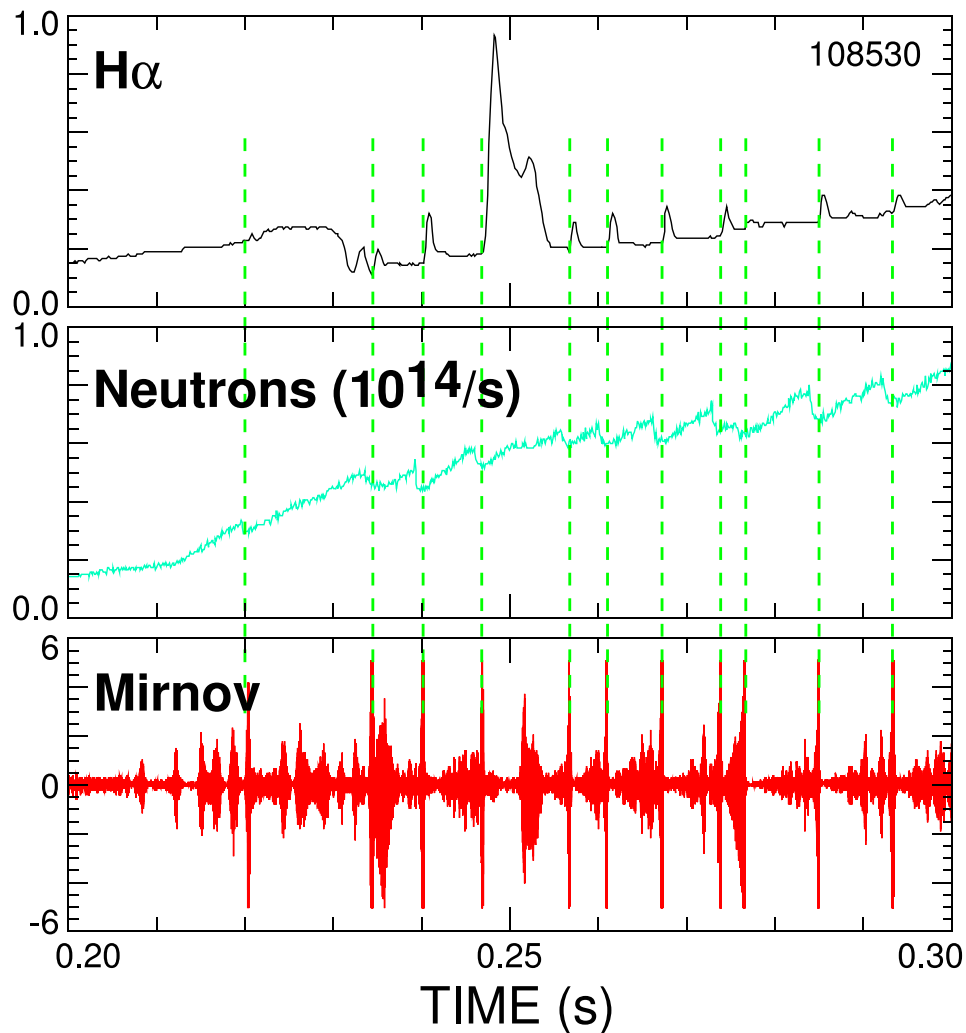
Typical growth rate is  $\gamma/\omega \simeq n_b/n_i \simeq 1\%$ .

Hybrid code “nonlinear” modeling will be covered in E. Belova talk today.



## Bursting TAEs in NSTX lead to neutron drop

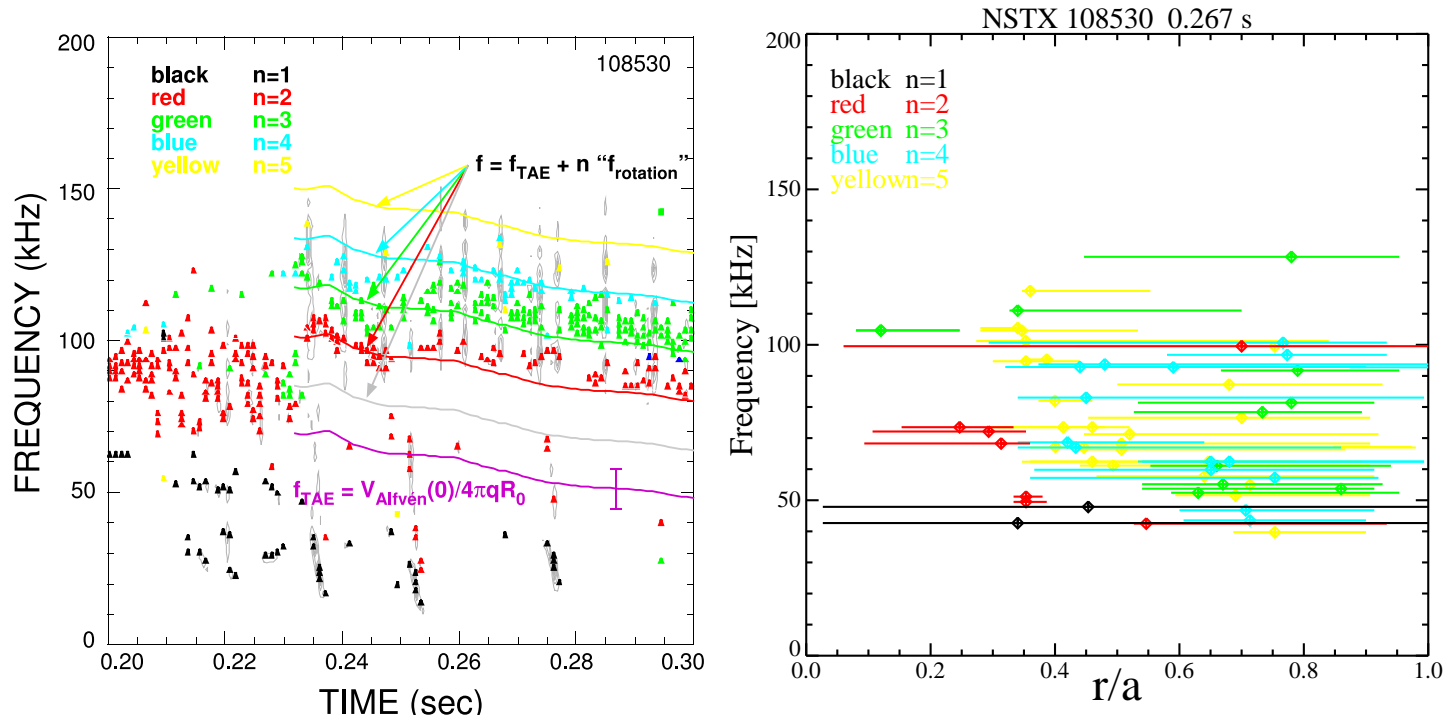
PPPL



- ✓ TAEs are bursting at  $t > 0.21msec$ .
- ✓ 5 – 10% of fast ions are lost during TAE bursts.
- ✓ NSTX shot with  $B = 0.434T$ ,  $R_0 = 87cm$ ,  $a = 63cm$ ,  $P = 3.2MW$ .
- ✓  $n = 1 - 5$  usually observed.
- ✓ burst time  $t \simeq 200\mu sec$ .
- ✓ see E. Fredrickson talk tomorrow.

# NOVA predicts frequencies of unstable TAEs in agreement with observations

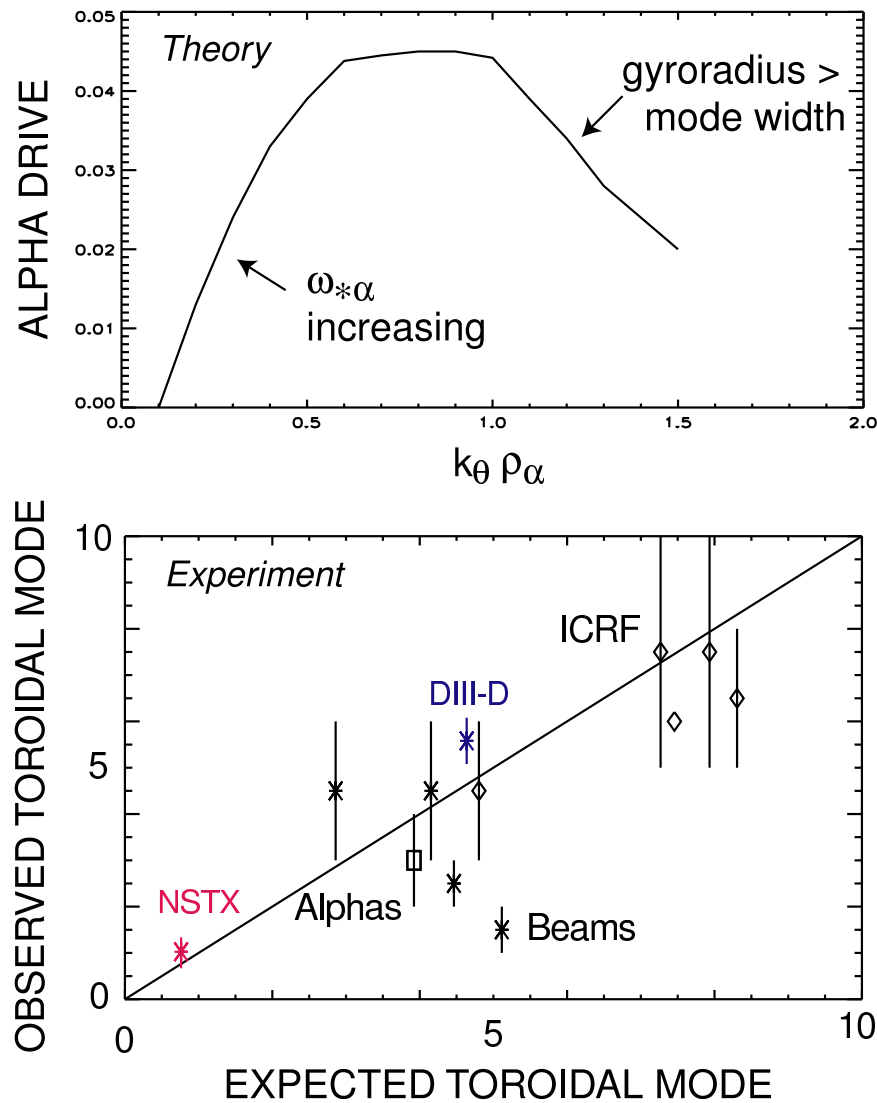
PPPL



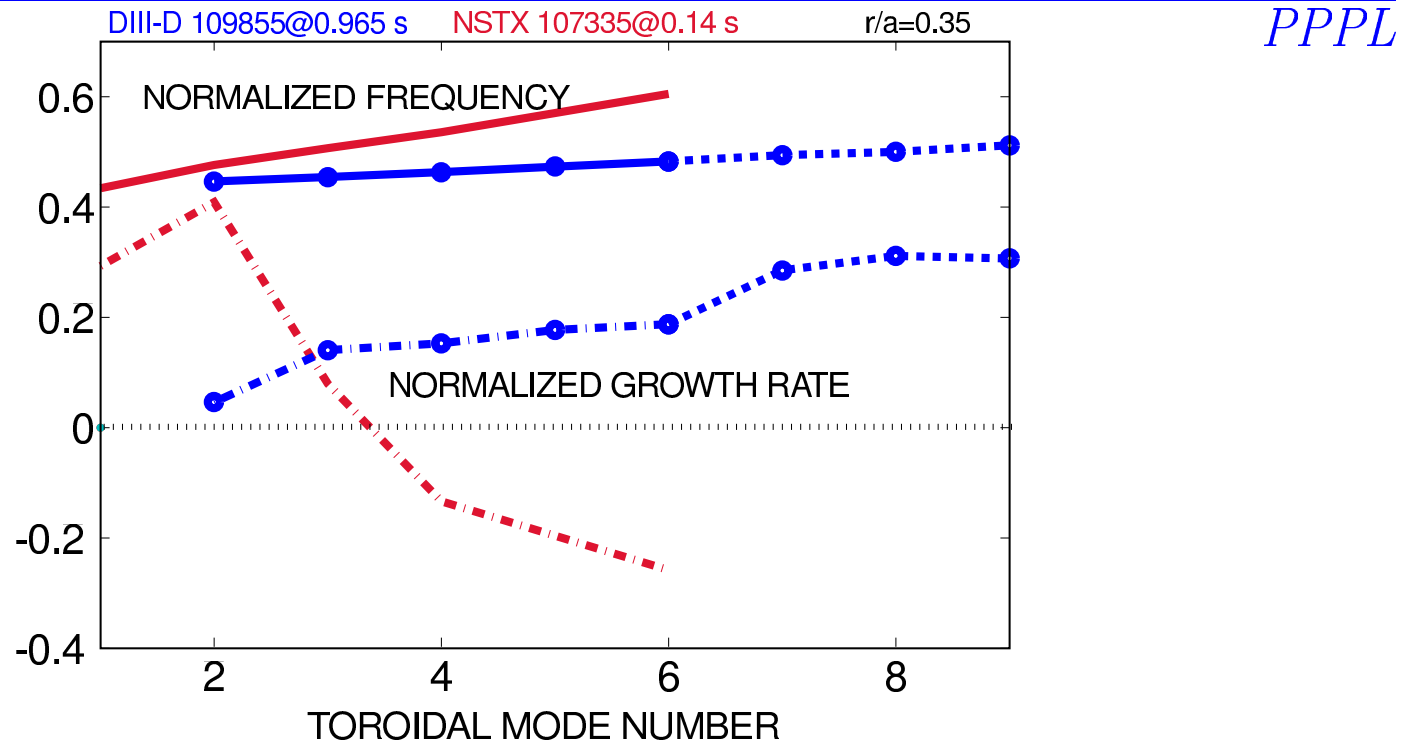
- ✓ Unstable TAEs with  $n = 1 - 5$ .
- ✓ High  $n$ 's are stabilized due to finite orbit width and Larmor radius.
- ✓ Growth rates are  $\gamma/\omega \simeq 1 - 4\%$ .
- ✓ Unstable modes are global and peaked at  $r/a \simeq 0.6$ .

# DIII-D/NSTX similarity experiment help to confirm burning plasma predictions (APS 2002, W. Heidbrink)

PPPL

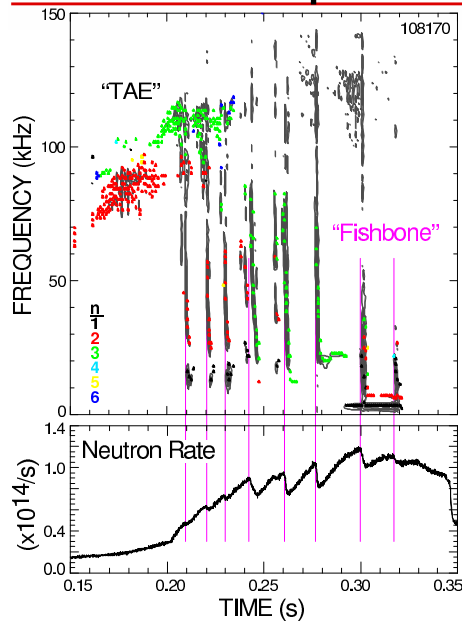


HINST predicts  $n = 2$  for NSTX;  $n \gtrsim 6$  for  
DIII-D



Confirms theory predictions for burning plasmas ITER, FIRE, IGNITOR.

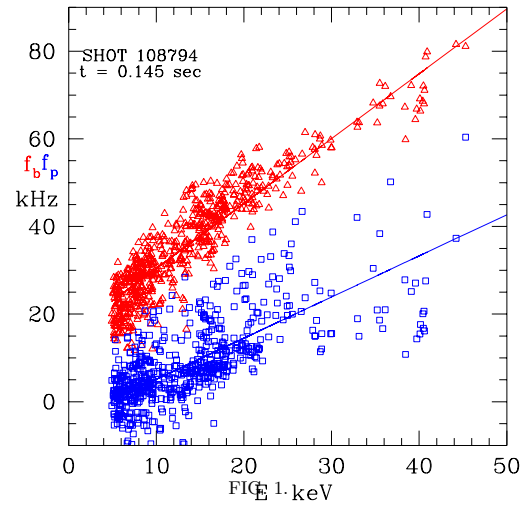
# Fishbones can cause large drops in neutron rate



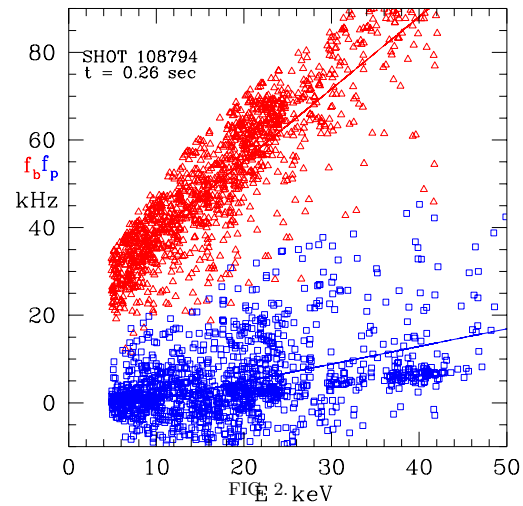
- Frequency chirps down rapidly
- $n=1, 2, 3$  mainly
- Thought to be bounce resonant
- $\Delta S_n \leq 25\%$
- Enhanced energetic neutral efflux seen at fishbones, sweeping from higher to lower energy with time

E. Fredrickson, R. White, S. Medley





Trapped particle bounce (red) and precession (blue) frequencies at  $t = 0.145\text{sec}$ .



Trapped particle bounce (red) and precession (blue) frequencies at  $t = 0.26\text{sec}$ .

*ORBIT code, R. White*

## Dispersion Relation

Assume  $m \simeq nq > 1$  and use the ballooning representation.  
Tsai and Chen (1993)

$$-i\frac{\omega}{\omega_A} + \delta W_f + \delta W_k = 0$$

$$\omega_A = v_A/qR$$

$$\delta W_k = \frac{\pi^2 e^2 q R_0 B_0}{m c^2 s} \int \frac{dE d\mu \theta_b^2 \Omega_d^2 \tau_b Q F_0}{\Delta_b (1 + \Delta_b^2)^{3/2}} \frac{\omega - n\omega_p}{\omega_b^2 - (\omega - n\omega_p)^2}$$

where  $E = v^2/2$ ,  $\mu = v_\perp^2/2B_0$ ,

$$\tau_b = 2\pi/\omega_b,$$

$$\Delta_b = (\theta_b k_\theta \rho_b)/2^{3/2} = \text{finite banana width effect.}$$

Here  $s = rq'/q$

$$QF_0 = (\omega \partial_E + \hat{\omega}_*)F_0$$

$$\hat{\omega}_*F_0 = \vec{k} \times \hat{e}_\parallel / \omega_c \cdot \nabla F_0.$$

Threshold when the drive due to the pressure inhomogeneity  $\hat{\omega}_*F_0$  at the  $\omega \simeq \omega_b$  wave bounce resonance exceeds the dissipation due to the Alfvén resonance absorption  $-i\omega/\omega_A$ .

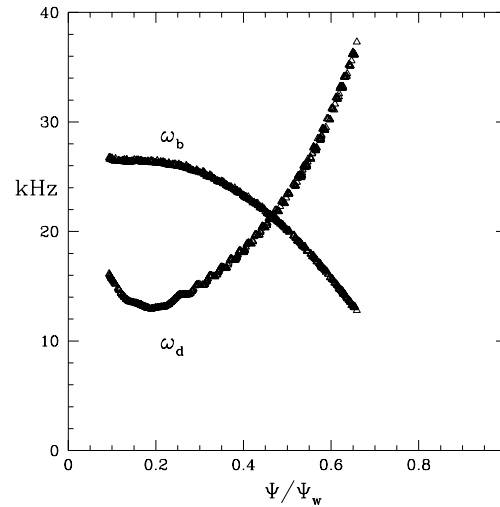
Slowing down distribution of single pitch,  $\delta W_f \simeq 0$

$$\omega = \omega_r + i\gamma, \quad \omega_r \simeq 0.83\omega_{bm}, \text{ and}$$

$$\frac{\gamma}{\omega_r} \simeq \frac{\pi}{8} \left( \frac{\alpha_E}{\alpha_{Ec}} - 1 \right)$$

where  $\alpha_E = q^2 R_0 \beta'_E$  and  $\alpha_{Ec} = 0.48 s \omega_{bm} / \theta_b \omega_A$

*L. Chen, R. White, APS 2002*



Bounce and Precession frequency vs  $\Psi$  for a 15 Kev ion.  
 Bounce angle  $\theta_b = 1.6$  as a function of poloidal flux.

For an MHD mode, there is a definite relation between radial motion and energy change,

$$d\psi = -mdE/\omega$$

### Outward motion corresponds to energy loss

- A particle resonating with  $\omega_d$  can stay in resonance as it moves out
- A particle resonating with  $\omega_b$  has difficulty staying in resonance as it moves out

*R. White, APS 2002*



## Conclusions

---

*PPPL*

1. Fast ion confinement in quiescent NSTX plasmas appears classical.
2. Sub-cyclotron oscillations in NSTX are identified as Compressional and/or Global Alfvén Eigenmode Instability driven by NBI ions.
3. GAE/CAEs may provide a channel for energy transfer from beam ions to thermal ions. Possible to explain thermal ion anomaly.
4. TAEs have significant effect on beam ion confinement.
5. Projection to DTST can be done basing on beam ion physics in NSTX.